Improved surface-wave retrieval from ambient seismic noise by multi-dimensional deconvolution

Kees Wapenaar,[1] Elmer Ruigrok,[1] Joost van der Neut,[1] and Deyan Draganov[1]

[1]   The methodology of surface-wave retrieval from ambient seismic noise by crosscorrelation relies on the assumption that the noise field is equipartitioned. Deviations from equipartitioning degrade the accuracy of the retrieved surface-wave Green's function. A point-spread function, derived from the same ambient noise field, quantifies the smearing in space and time of the virtual source of the Green's function. By multidimensionally deconvolving the retrieved Green's function by the point-spread function, the virtual source becomes better focussed in space and time and hence the accuracy of the retrieved surface-wave Green's function may improve significantly. We illustrate this at the hand of a numerical example and discuss the advantages and limitations of this new methodology. **Citation:** Wapenaar, K., E. Ruigrok, J. van der Neut, and D. Draganov (2011), Improved surface-wave retrieval from ambient seismic noise by multi-dimensional deconvolution, *Geophys. Res. Lett.*, *38*, L01313, doi:10.1029/2010GL045523.

1.   Introduction

[2]   The possibility to retrieve surface waves from ambient seismic noise, as pioneered by *Campillo and Paul* [2003], *Shapiro and Campillo* [2004] and *Sabra et al.* [2005b], has led to many successful applications in tomographic imaging of the earth's crust at different scales [*Sabra et al.*, 2005a; *Gerstoft et al.*, 2006; *Yao et al.*, 2006; *Bensen et al.*, 2007; *Liang and Langston*, 2008; *Ma et al.*, 2008; *Lin et al.*, 2009; *Picozzi et al.*, 2009]. The basic principle is very simple: assuming the ambient noise field is equipartitioned and the medium is lossless, the crosscorrelation of noise observations at two seismometers converges to the Green's function between these seismometers. Although it follows from theory that the full Green's function can be obtained [*Wapenaar*, 2004; *Halliday and Curtis*, 2008], in most practical situations only the fundamental mode of the direct surface wave is retrieved. Moreover, because the condition of equipartitioning is usually not fulfilled, the accuracy of the retrieved surface waves is limited, which may lead to errors in the estimated traveltimes and hence in the velocity model obtained by tomographic inversion. Several approaches have been proposed to compensate for deviations from equipartitioning, each with its own advantages and limitations. *Stehly et al.* [2008] show that in a strongly scattering environment, anisotropic illumination by the primary sources can be partly remedied by taking the crosscorrelation of the coda of the crosscorrelation. For exploration-type applications,

Schuster and Zhou [2006] and *Wapenaar et al.* [2008] proposed Green's function retrieval by "multidimensional deconvolution" (MDD) as an alternative to the crosscorrelation method. *Curtis and Halliday* [2010] deconvolve the crosscorrelation by the estimated radiation pattern of the virtual source in a method they call "directional balancing".

[3]   The concept of Green's function retrieval by MDD is based on inverting an exact convolutional Green's function representation [*Wapenaar and van der Neut*, 2010] and circumvents the main underlying assumptions of the correlation method (equipartitioning and absence of loss) in a natural way. Here we show with a numerical example that MDD has the potential to significantly improve surface-wave retrieval from ambient noise.

2.   Modeling of Ambient-Noise Surface Waves

[4]   Consider the configuration of Figure 1, which shows a map of the USA, a number of receiver stations of the USArray (green triangles) and a number of sources along the East coast (blue dots), for example representing storm-related microseismic sources [*Bromirski*, 2001]. Note that the source distribution is irregular, containing two dense clusters embedded in a somewhat sparser background distribution. Assuming a layered crust, we compute the dispersion curve of the fundamental mode of the Rayleigh-wave for the upper 300 km of the PREM model [*Dziewonski and Anderson*, 1981], using the approach described by *Wathelet et al.* [2004]. The dispersion curve is shown Figure 1a. We define the sources as simultaneously acting uncorrelated noise sources, with a period band of 15 to 50 s, which entails the single-frequency microseism. Using the computed dispersion curve, we model the surface-wave response of the distribution of noise sources at all indicated stations. Figures 1b and 1c show 25 minutes of the responses along the East–West and North–South arrays, respectively (the total duration of the modeled noise responses is approximately two days).

3.   Surface-Wave Retrieval by Crosscorrelation

[5]   We define the crosscorrelation of two noise responses $u(\mathbf{x}_A, t)$ and $u(\mathbf{x}_B, t)$ at two stations $\mathbf{x}_A$ and $\mathbf{x}_B$ as

$$C(\mathbf{x}_B, \mathbf{x}_A, t) = \langle u(\mathbf{x}_B, t) * u(\mathbf{x}_A, -t) \rangle. \qquad (1)$$

The asterisk stands for convolution; the time-reversal of one of the responses turns the convolution into a correlation. The notation $\langle \cdot \rangle$ stands for ensemble averaging, which is in practice replaced by integrating over sufficiently long time and/or averaging over different time intervals.

[6]   Our aim is to turn one of the stations of the North–South array (the one indicated by the red dot in Figure 1) into a virtual source and to retrieve the response of this virtual

[1]Department of Geotechnology, Delft University of Technology, Delft, Netherlands.
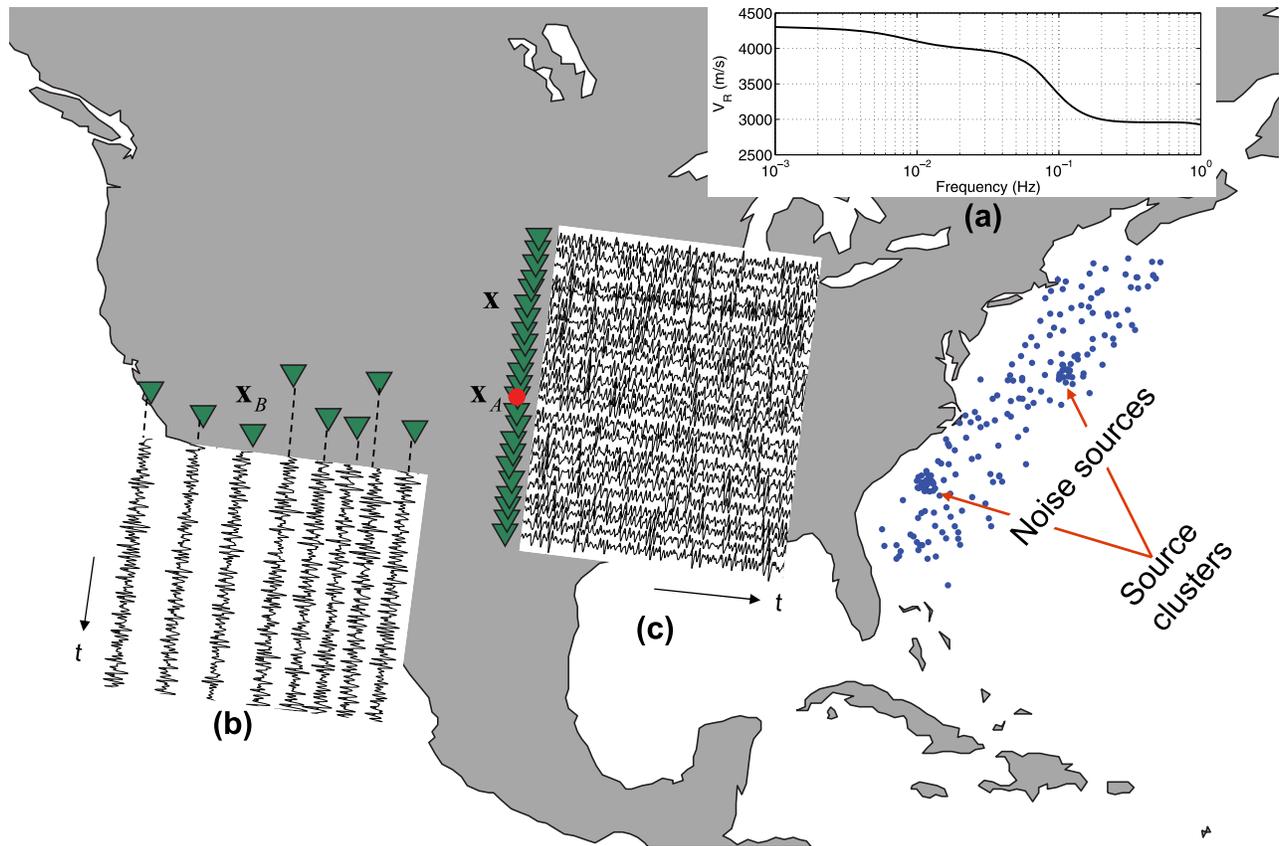
Figure 1. Configuration for numerical ambient-noise modeling. The background shows a map of the USA with two arrays of receiver stations (green triangles) and an irregular distribution of noise sources along the East coast (blue dots). (a) Dispersion curve of the fundamental Rayleigh-wave mode. (b) 25 minutes of the modeled noise response along the East–West array. (c) Idem, along the North–South array.

source at the receiver stations along the East–West array. Following the crosscorrelation method, we take the noise response in Figure 1c at the station indicated by the red dot and crosscorrelate it with each of the responses at the stations of the East–West array (Figure 1b). Hence, we evaluate equation (1), with $\mathbf{x}_A$ fixed at the red dot and $\mathbf{x}_B$ variable along the East–West array. The correlation function $C(\mathbf{x}_B, \mathbf{x}_A, t)$ is shown in Figure 2a by the red traces. For comparison, the black traces in Figure 2a represent the directly modeled surface-wave Green's function with its source at the position of the red dot, convolved with a source function $S(t)$ equal to the average autocorrelation of the noise. According to the theory, the correlation function should consist of the Green's function and its time-reversed version, but here we retrieved a causal contribution only. The explanation for this is that the distribution of sources is restricted to the East coast and hence is not enclosing the receiver stations (i.e., one of the conditions for equipartitioning is violated). The absence of an acausal contribution is not a severe drawback, as long as the causal contribution is accurate. Looking at the causal contribution we observe that, although the travel times seem to match reasonably well, some of the seismograms show a small travel time error (see Figure 2b). This leads to velocity errors in the order of one percent in the retrieved dispersion curve, see Figure 2c. This is not small compared to the velocity shifts that are inverted for in surface-wave inversion

(several percent). There is also a pronounced mismatch between the amplitudes of the red and black waveforms in Figure 2b. The travel time and amplitude perturbations are a result of the irregularity of the source distribution. The effect of the source irregularity on the retrieved response is quantified mathematically in the next section.

[7] Although we applied the crosscorrelation method to numerically modeled data, the results are representative for real data situations. *Bensen et al.* [2007] processed ambient noise observed by USArray stations. *Bensen et al.* [2007, Figure 15] compare noise crosscorrelations with direct earthquake observations. *Bensen et al.* [2007, Figure 17] show a comparison of retrieved dispersion curves with a modeled prediction. The mismatches in our Figures 2b and c are in the same range as those in Figures 15 and 17 of *Bensen et al.* [2007].

4. The Point-Spread Function

[8] *Van der Neut et al.* [2010] and *Wapenaar and van der Neut* [2010] introduce a point-spread function, defined as

$$\Gamma(\mathbf{x}, \mathbf{x}_A, t) = \langle u(\mathbf{x}, t) * u(\mathbf{x}_A, -t) \rangle. \qquad (2)$$

Note that this definition looks very similar to that of the correlation function (equation (1)), except that the involved
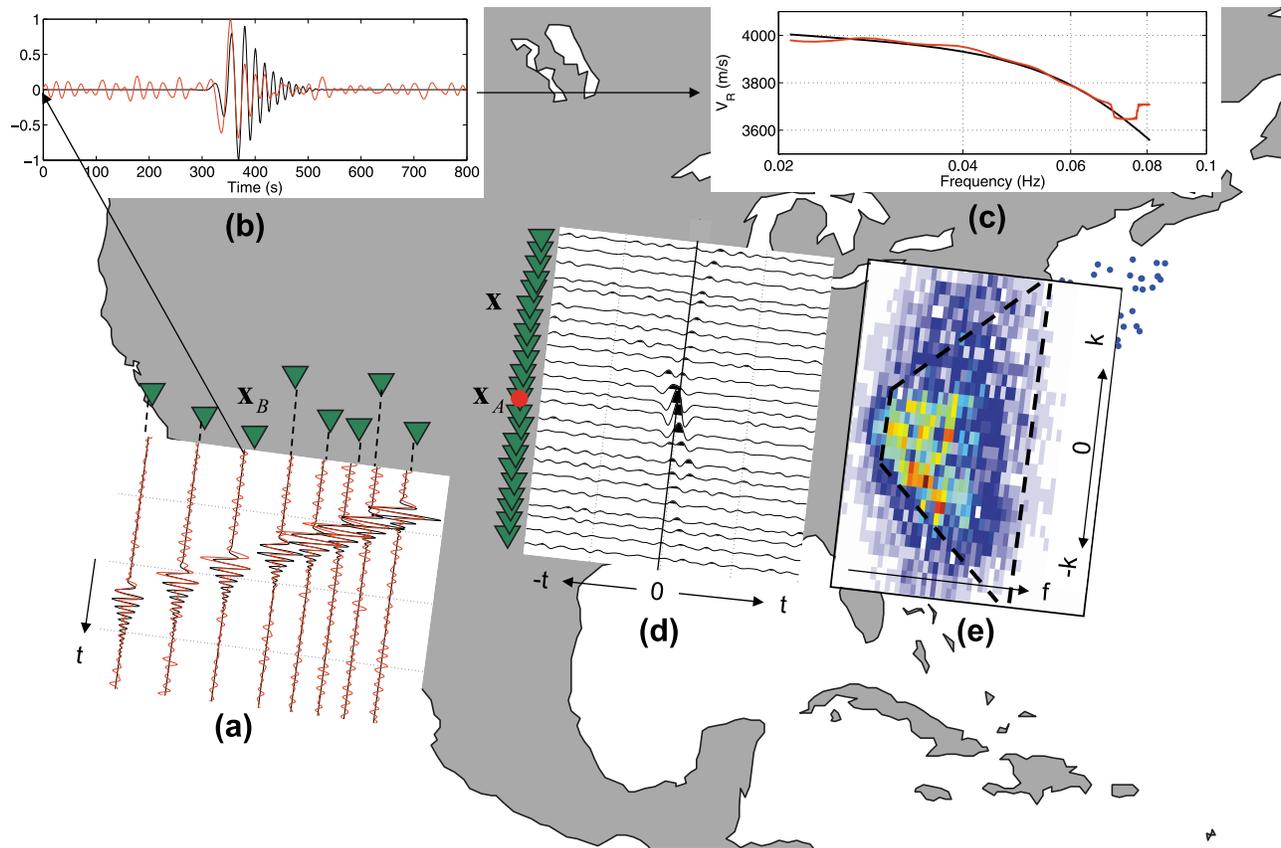
Figure 2. Surface-wave retrieval by crosscorrelation. (a) Red traces: result of crosscorrelating the noise recording in Figure 1c at the station indicated by the red dot with each of the noise recordings along the East–West array in Figure 1b. Black traces: for comparison, the directly modeled surface-wave response of a source at the position of the red dot, convolved with the average autocorrelation $S(t)$ of the noise. (b) Zoomed version of one of the traces in Figure 2a. (c) Retrieved dispersion curve (red), compared with the modeled dispersion curve (black). (d) Point-spread function, obtained by crosscorrelating the noise in Figure 1c recorded at the station indicated by the red dot with each of the noise recordings along the North–South array in that figure. (e) Wavenumber-frequency spectrum of the point-spread function in Figure 2d.

stations $\mathbf{x}$ and $\mathbf{x}_A$ are chosen differently. For the configuration we are considering, $\mathbf{x}$ and $\mathbf{x}_A$ are both chosen on the North–South array. By taking $\mathbf{x}_A$ fixed at the red dot and $\mathbf{x}$ variable along the same array, we obtain the point-spread function $\Gamma(\mathbf{x}, \mathbf{x}_A, t)$, shown in Figure 2d. Note that most energy is focused around $\mathbf{x} = \mathbf{x}_A$ and $t = 0$, but the focus is not very sharp. The smearing of this focused energy over space and time is a result of the irregularity of the source distribution. If the source distribution were regular, the point-spread function would converge to a sharper focus at $\mathbf{x} = \mathbf{x}_A$ and $t = 0$. Figure 2e is the wavenumber-frequency spectrum of the point-spread function. It exhibits significant irregular deviations from a flat spectrum as a result of the irregular source distribution. The cut-off at large wavenumbers (i.e., beyond the slanted dashed lines) is a result of the finite source aperture.

[9] It can be shown that the correlation function $C(\mathbf{x}_B, \mathbf{x}_A, t)$, the point-spread function $\Gamma(\mathbf{x}, \mathbf{x}_A, t)$ and the dipole Green's function $G_{\mathrm{d}}(\mathbf{x}_B, \mathbf{x}, t)$ are mutually related as follows

$$C(\mathbf{x}_B, \mathbf{x}_A, t) = \int_{\mathbb{S}} G_{\mathrm{d}}(\mathbf{x}_B, \mathbf{x}, t) * \Gamma(\mathbf{x}, \mathbf{x}_A, t) \mathrm{d}\mathbf{x} \quad (3)$$

[van der Neut et al., 2010; Wapenaar and van der Neut, 2010]. For the considered configuration, the integration boundary $\mathbb{S}$ corresponds to the North–South array. Equation (3) shows that the correlation function is proportional to the Green's function with its source smeared in space and time by the point-spread function. Hence, the retrieved surface-wave response in Figure 2a can be interpreted as the response of an extended virtual source around the red dot, with its space-time behavior defined by the point-spread function shown in Figure 2d.

5. Surface-Wave Retrieval by Multidimensional Deconvolution (MDD)

[10] In order to retrieve the surface-wave response of a virtual source focused at the red dot we need to remove the imprint of the point-spread function from the correlation function. In other words, we need to invert equation (3) for the Green's function $G_{\mathrm{d}}(\mathbf{x}_B, \mathbf{x}, t)$ (for $\mathbf{x} = \mathbf{x}_A$) by deconvolving the correlation function $C(\mathbf{x}_B, \mathbf{x}_A, t)$ by the point-spread function $\Gamma(\mathbf{x}, \mathbf{x}_A, t)$. The spectrum in Figure 2e shows that this deconvolution process is necessarily band-limited. For the inversion of equation (3), the integral needs to be
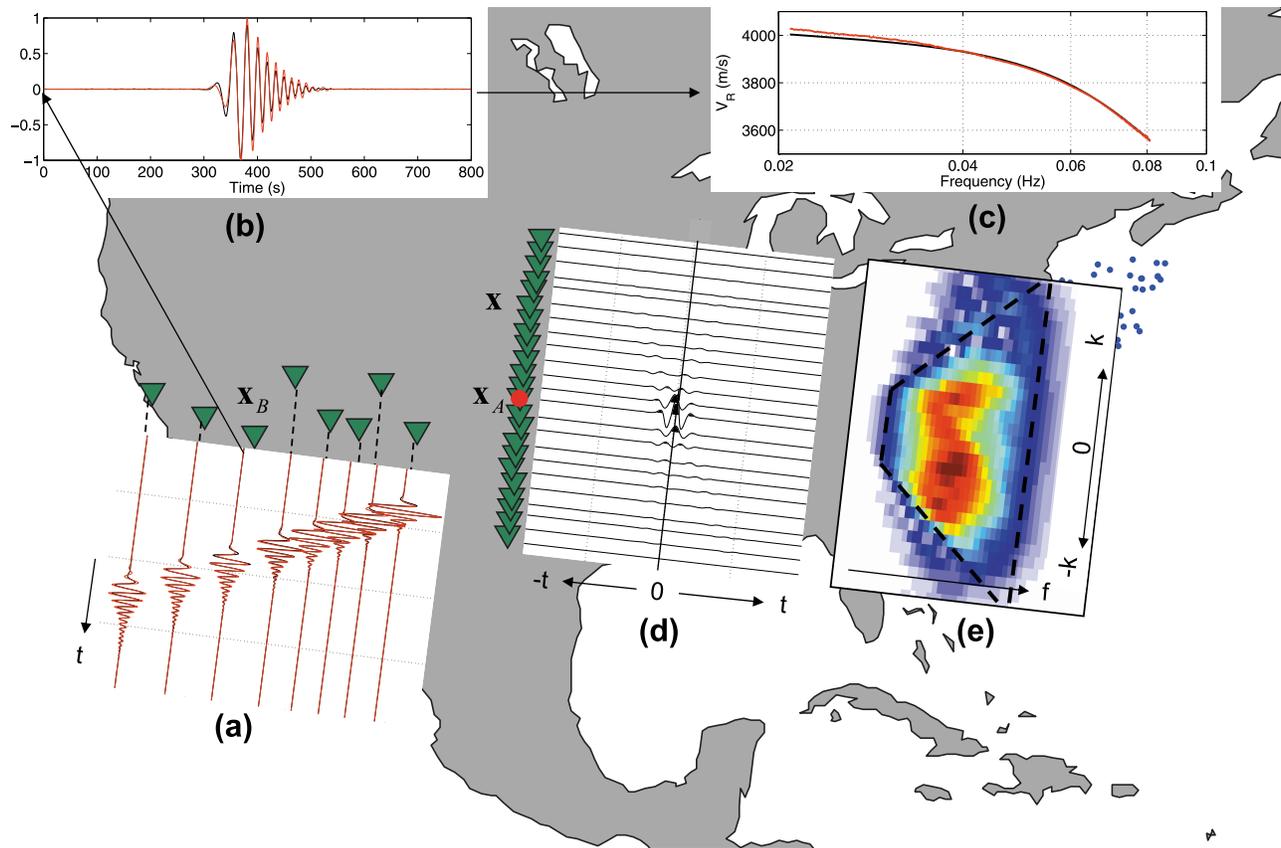
Figure 3. Surface-wave retrieval by multidimensional deconvolution (MDD). (a) Red traces: result of multidimensionally deconvolving the responses in Figure 2a by the point-spread function in Figure 2d. Black traces: the directly modeled surface-wave response of a source at the position of the red dot. (b) Zoomed version of one of the traces in Figure 3a. (c) Retrieved dispersion curve (red), compared with the modeled dispersion curve (black). (d) Focused virtual source. (e) Wavenumber-frequency spectrum of the virtual source in Figure 3d.

discretized (which assumes that the North–South array is regularly sampled with at least two stations per apparent wavelength). Next, by transforming the correlation function and the point-spread function to the frequency domain (for all $\mathbf{x}$ and $\mathbf{x}_A$ along the North–South array), equation (3) becomes a matrix equation for each frequency component, i.e., $\mathbf{C} = \mathbf{G}_d\mathbf{\Gamma}$. This can be solved for the frequency-domain Green's function $\mathbf{G}_d$ by matrix inversion of the point-spread function $\mathbf{\Gamma}$. We stabilize this inversion by adding a small constant ε^2 to the diagonal of this matrix, hence $\mathbf{G}_d = \mathbf{C}(\mathbf{\Gamma} + \varepsilon^2\mathbf{I})^{-1}$, where $\mathbf{I}$ is the identity matrix. Transforming the end-result back to the time domain gives a band-limited estimate of the Green's function $G_d(\mathbf{x}_B, \mathbf{x}_A, t)$, which completes the MDD process. The result is shown by the red traces in Figure 3a for fixed $\mathbf{x}_A$ (the red dot) and variable $\mathbf{x}_B$ (the stations along the East–West array). For ease of comparison, the retrieved Green's function has been convolved with the average autocorrelation function $S(t)$. Note that the match with the directly modeled response (the black traces) is excellent (see also Figure 3b). Moreover, the retrieved dispersion curve is very accurate, except for very low frequencies (Figure 3c). The virtual source of the retrieved response is shown in Figure 3d. It has been obtained by applying the band-limited inverse point-spread function to the point-spread function itself, followed by a convolution with $S(t)$. Note that this source is much better focused than the one in

Figure 2d. Figure 3e shows the wavenumber-frequency spectrum of the focused source. Apart from the imprint of $S(t)$ it is almost flat within the bounds determined by the source aperture and the temporal bandwidth of the sources.

6. Concluding Remarks

[11] We have shown that the surface-wave Green's function, retrieved from ambient noise by crosscorrelation, can be improved by MDD, i.e., by deconvolving the correlation function by the point-spread function.

[12] MDD requires that the point-spread function can be computed. Similar as the correlation function, the point-spread function is directly obtained from noise observations (compare equation (2) with (1)), hence, no explicit knowledge is required of the sources and the medium parameters. However, unlike the correlation function, which can be obtained from any combination of two stations, computation of the point-spread function and its inverse requires a regular and well-sampled array of stations. Moreover, whereas the correlation method is a simple trace-by-trace process, MDD involves an inversion of an integral equation, which in practice is achieved by matrix inversion. Apart from the higher cost (in comparison with the correlation method), this matrix inversion can be unstable. The well-posedness of this inverse problem depends on the number of available

sources, the source aperture and the bandwidth. As demonstrated in the example, a spectral analysis of the point-spread function helps to assess for which spatial and temporal frequencies the inversion can be carried out in a stable sense.

[13]   In the example we have considered a layered medium, hence no scattering takes place in the lateral direction. This is not a fundamental restriction of the method. When scattering plays a role, equations (1)–(3) are still valid, except that $u(\mathbf{x}_A, t)$ in equation (1) and both fields in equation (2) (hence, all fields on $\mathbb{S}$), should be replaced by inward propagating fields on $\mathbb{S}$ ("inward" into the domain of interest, which is the area West of the North–South array in our example) [*Wapenaar and van der Neut*, 2010]. Retrieving the inward propagating field from the total field requires decomposition, which is possible when multicomponent data are available or when there are parallel receiver arrays close to each other. This decomposition would also be required when sources were present at both sides of the arrays. Alternatively, when the scattering is not too strong, the "decomposed" correlation function and point-spread function can be obtained from the correlation function of the full wave fields by means of time-windowing (in the correlation-time domain). In any case, the point-spread function will be more complex in the presence of scattering and hence stabilization of the matrix inversion should be done with care. *Wapenaar and van der Neut* [2010] discuss a seismic exploration-type application of MDD and demonstrate that a carefully inverted point-spread function properly suppresses the scattering artifacts.

[14]   With a numerical example we have demonstrated the potential of MDD to improve the retrieval of surface-wave Green's functions from ambient noise. MDD not only ensures that the phase and amplitude of the recovered surface waves are correct, it also suppresses the fluctuations in Figures 2a and 2b that are caused by the sparse and irregular distribution of the noise sources. Surface-wave Green's functions obtained by MDD will lead to improved passive tomographic inversion, which is relevant for imaging the velocity model of the earth's crust, monitoring post-seismic relaxation, monitoring changes in volcanic interiors, etc.

References

Bensen, G. D., M. H. Ritzwoller, M. P. Barmin, A. L. Levshin, F. Lin, M. P. Moschetti, N. M. Shapiro, and Y. Yang (2007), Processing seismic ambient noise data to obtain reliable broad-band surface wave dispersion measurements, *Geophys. J. Int.*, *169*, 1239–1260.

Bromirski, P. D. (2001), Vibrations from the "Perfect Storm", *Geochem. Geophys. Geosyst.*, *2*, 1030, doi:10.1029/2000GC000119.

Campillo, M., and A. Paul (2003), Long-range correlations in the diffuse seismic coda, *Science*, *299*, 547–549.

Curtis, A., and D. Halliday (2010), Directional balancing for seismic and general wavefield interferometry, *Geophysics*, *75*(1), SA1–SA14.

Dziewonski, A. M., and D. L. Anderson (1981), Preliminary reference Earth model, *Phys. Earth Planet. Inter.*, *25*, 297–356.

Gerstoft, P., K. G. Sabra, P. Roux, W. A. Kuperman, and M. C. Fehler (2006), Green's functions extraction and surface-wave tomography from microseisms in southern California, *Geophysics*, *71*(4), SI23–SI31.

Halliday, D., and A. Curtis (2008), Seismic interferometry, surface waves and source distribution, *Geophys. J. Int.*, *175*, 1067–1087.

Liang, C., and C. A. Langston (2008), Ambient seismic noise tomography and structure of eastern North America, *J. Geophys. Res.*, *113*, B03309, doi:10.1029/2007JB005350.

Lin, F.-C., M. H. Ritzwoller, and R. Snieder (2009), Eikonal tomography: Surface wave tomography by phase front tracking across a regional broad-band seismic array, *Geophys. J. Int.*, *177*, 1091–1110.

Ma, S., G. A. Prieto, and G. C. Beroza (2008), Testing community velocity models for southern California using the ambient seismic field, *Bull. Seismol. Soc. Am.*, *98*, 2694–2714.

Picozzi, M., S. Parolai, D. Bindi, and A. Strollo (2009), Characterization of shallow geology by high-frequency seismic noise tomography, *Geophys. J. Int*, *176*, 164–174.

Sabra, K. G., P. Gerstoft, P. Roux, W. A. Kuperman, and M. C. Fehler (2005a), Surface wave tomography from microseisms in southern California, *Geophys. Res. Lett.*, *32*, L14311, doi:10.1029/2005GL023155.

Sabra, K. G., P. Gerstoft, P. Roux, W. A. Kuperman, and M. C. Fehler (2005b), Extracting time-domain Green's function estimates from ambient seismic noise, *Geophys. Res. Lett.*, *32*, L03310, doi:10.1029/2004GL021862.

Schuster, G. T., and M. Zhou (2006), A theoretical overview of model-based and correlation-based redatuming methods, *Geophysics*, *71*(4), SI103–SI110.

Shapiro, N. M., and M. Campillo (2004), Emergence of broadband Rayleigh waves from correlations of the ambient seismic noise, *Geophys. Res. Lett.*, *31*, L07614, doi:10.1029/2004GL019491.

Stehly, L., M. Campillo, B. Froment, and R. L. Weaver (2008), Reconstructing Green's function by correlation of the coda of the correlation (C^3) of ambient seismic noise, *J. Geophys. Res.*, *113*, B11306, doi:10.1029/2008JB005693.

van der Neut, J., E. Ruigrok, D. Draganov, and K. Wapenaar (2010), Retrieving the earth's reflection response by multi-dimensional deconvolution of ambient seismic noise, paper presented at the 72nd Annual International EAGE Meeting, Barcelona, Spain.

Wapenaar, K. (2004), Retrieving the elastodynamic Green's function of an arbitrary inhomogeneous medium by cross correlation, *Phys. Rev. Lett.*, *93*, 254301, doi:10.1103/PhysRevLett.93.254301.

Wapenaar, K. and J. van der Neut (2010), A representation for Green's function retrieval by multidimensional deconvolution, *J. Acoust. Soc. Am.*, *128*(6), EL366–EL371, doi:10.1121/1.3509797.

Wapenaar, K., J. van der Neut, and E. Ruigrok (2008), Passive seismic interferometry by multi-dimensional deconvolution, *Geophysics*, *73*(6), A51–A56.

Wathelet, M. D., D. Jongmans, and M. Ohrnberger (2004), Surface-wave inversion using a direct search algorithm and its application to ambient vibration measurements, *Near Surf. Geophys.*, *2*, 211–221.

Yao, H., R. D. van der Hilst, and M. V. de Hoop (2006), Surface-wave array tomography in SE Tibet from ambient seismic noise and two-station analysis—I. Phase velocity maps, *Geophys. J. Int.*, *166*, 732–744.

D. Draganov, E. Ruigrok, J. van der Neut, and K. Wapenaar, Department of Geotechnology, Delft University of Technology, PO Box 5048, NL-2600 GA Delft, Netherlands. (d.s.draganov@tudelft.nl; e.n.ruigrok@tudelft.nl; j.r.vanderneut@tudelft.nl; c.p.a.wapenaar@tudelft.nl)